Supporting Information

Ternary Polymer-Perylenediimide-Carbon Nanotube Photovoltaics with High Efficiency and Stability under Super-Solar Irradiation

Authors: Tejas A. Shastry[1,3], Patrick E. Hartnett[2,3], Michael R. Wasielewski[2,3], Tobin J. Marks[1,2,3], and Mark C. Hersam[1,2,3,*]

[1]Department of Materials Science and Engineering, Northwestern University, Evanston, IL 60208, United States.

[2]Department of Chemistry, Northwestern University, Evanston, IL 60208, United States.

[3]Argonne-Northwestern Solar Energy Research Center, Northwestern University, Evanston, IL 60208, United States.

*Correspondence to: m-hersam@northwestern.edu

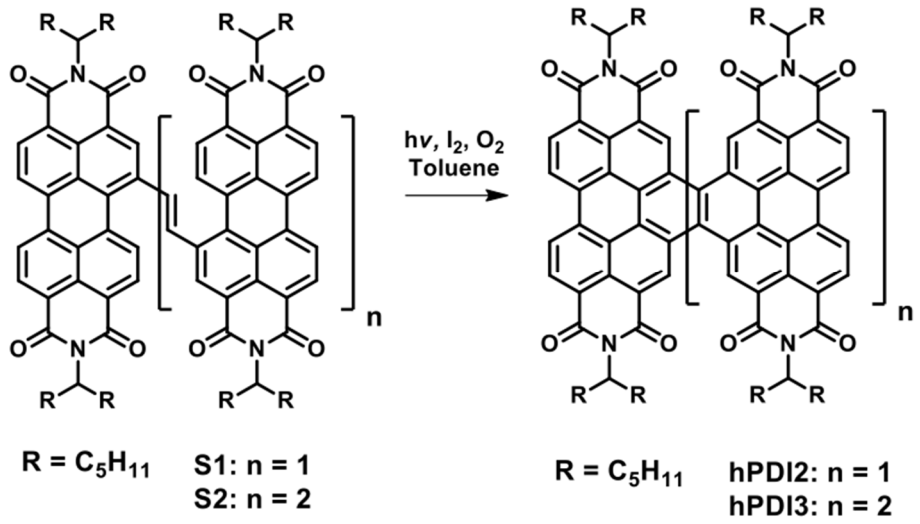

Figure S1. Reaction scheme for helical hPDI2 and hPDI3 acceptors.

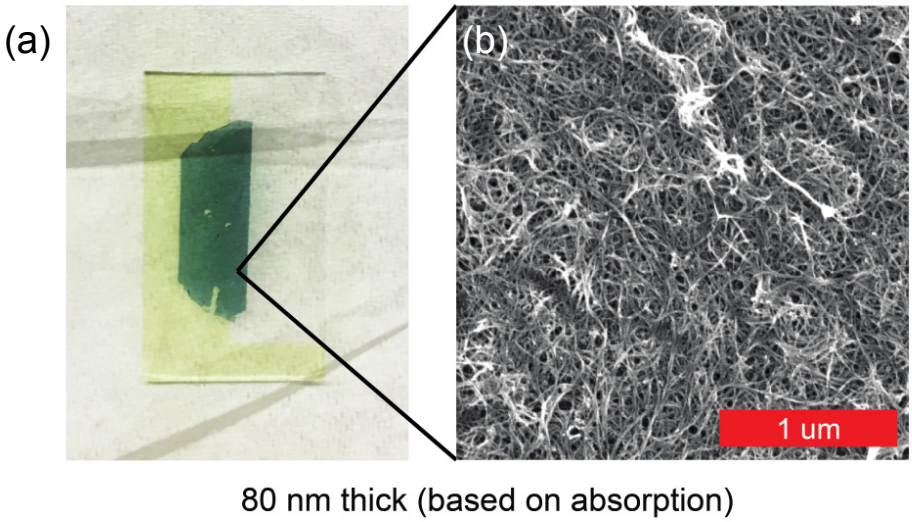

Figure S2. (a) Photograph of transferred film of semiconducting (7,6) SWCNTs on ITO-coated glass. (b) Scanning electron micrograph of the SWCNT film shown in (a).

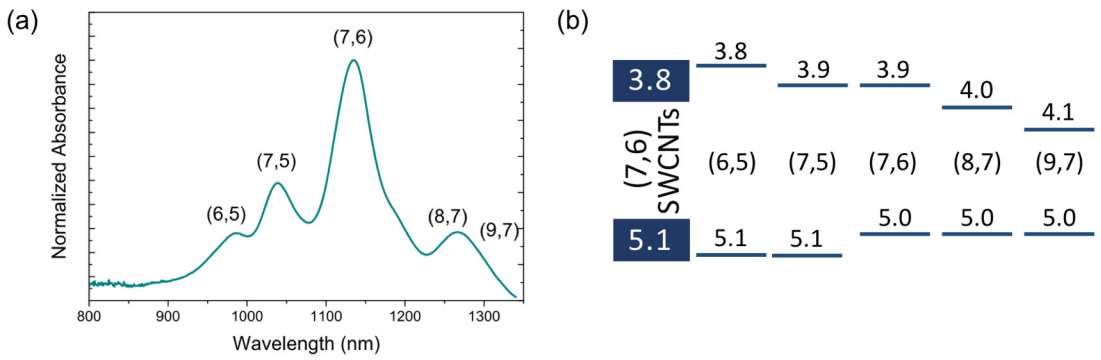

Figure S3. (a) Optical absorbance spectrum with assigned chiralities and (b) band gaps and conduction and valence band offsets of semiconducting SWCNTs, as per previously published values.[1] Values for band gaps are presented with units of eV.

Table S1. Summary of chiralities for the semiconducting (7,6) SWCNTs shown in Figure S1.

Chirality	% of distribution	Band gap (eV)	Conduction band (eV)	Valence band (eV)
(6,5)	12%	1.3	3.8	5.1
(7,5)	25%	1.2	3.9	5.1
(7,6)	51%	1.1	3.9	5.0
(8,7)	12%	1.0	4.0	5.0
(9,7)	2%	0.9	4.1	5.0

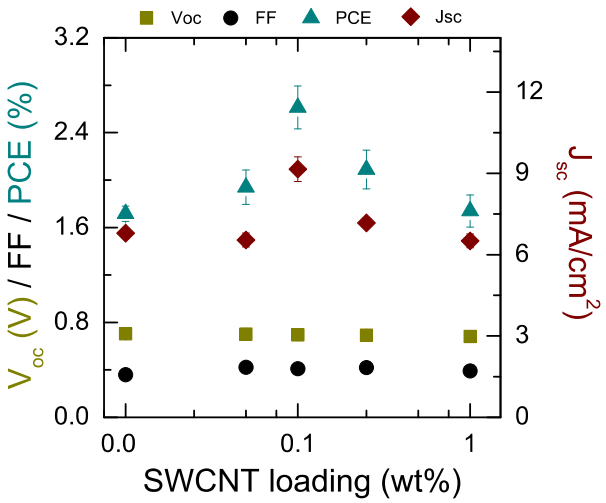

Figure S4. Dependence of photovoltaic performance parameters on the loading of semiconducting SWCNTs in PTB7-hPDI2 blends.

Table S2. Summary of photovoltaic parameters of PTB7-hPDI2 solar cells with various loadings of semiconducting SWCNTs. Champion values listed in [brackets].

s-SWCNT loading (wt%)	Voc (V)	Jsc (mA/cm^2)	FF (%)	PCE (%)
0.00	0.70 ± 0.01 [0.72]	6.77 ± 0.15 [6.87]	35.9 ± 1.7 [42.9]	1.72 ± 0.06 [2.1]
0.05	0.70 ± 0.01 [0.72]	6.54 ± 0.26 [6.91]	42.2 ± 1.2 [43.8]	1.94 ± 0.15 [2.2]
0.10	0.70 ± 0.01 [0.73]	9.17 ± 0.46 [9.78]	41.0 ± 1.6 [42.7]	2.61 ± 0.18 [3.0]
0.25	0.69 ± 0.02 [0.72]	7.17 ± 0.17 [7.39]	42.0 ± 1.8 [44.7]	2.09 ± 0.16 [2.4]
1.00	0.68 ± 0.02 [0.70]	6.51 ± 0.25 [6.94]	39.1 ± 1.3 [41.4]	1.74 ± 0.14 [2.0]

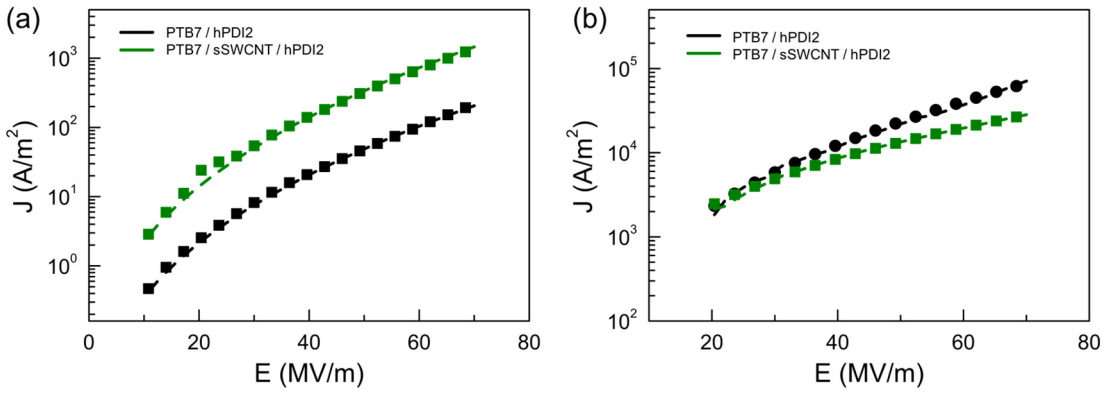

Figure S5. Current density versus applied field for (a) electron only and (b) hole only devices of PTB7-hPDI2 and ternary PTB7-SWCNT-hPDI2 blends.

Table S3. Summary of electron and hole mobility (μ_0) and field dependence coefficient (γ) extracted from electron and hole devices of PTB7-hPDI2 and ternary PTB7-SWCNT-hPDI2 blends.

	Electron Mobility		Hole Mobility	
	μ_0 (cm^2/Vs)	γ ($m^{1/2}V^{-1/2}$)	μ_0 (cm^2/Vs)	γ ($m^{1/2}V^{-1/2}$)
PTB7-hPDI2	$(4.0 \pm 0.1) * 10^{-5}$	$(8.5 \pm 0.2) * 10^{-4}$	$(1.6 \pm 0.2) * 10^{-4}$	$(5.5 \pm 0.2) * 10^{-4}$
PTB7-SWCNT-hPDI2	$(2.4 \pm 0.1) * 10^{-4}$	$(8.7 \pm 0.2) * 10^{-4}$	$(5.0 \pm 0.1) * 10^{-4}$	$(3.1 \pm 0.3) * 10^{-4}$

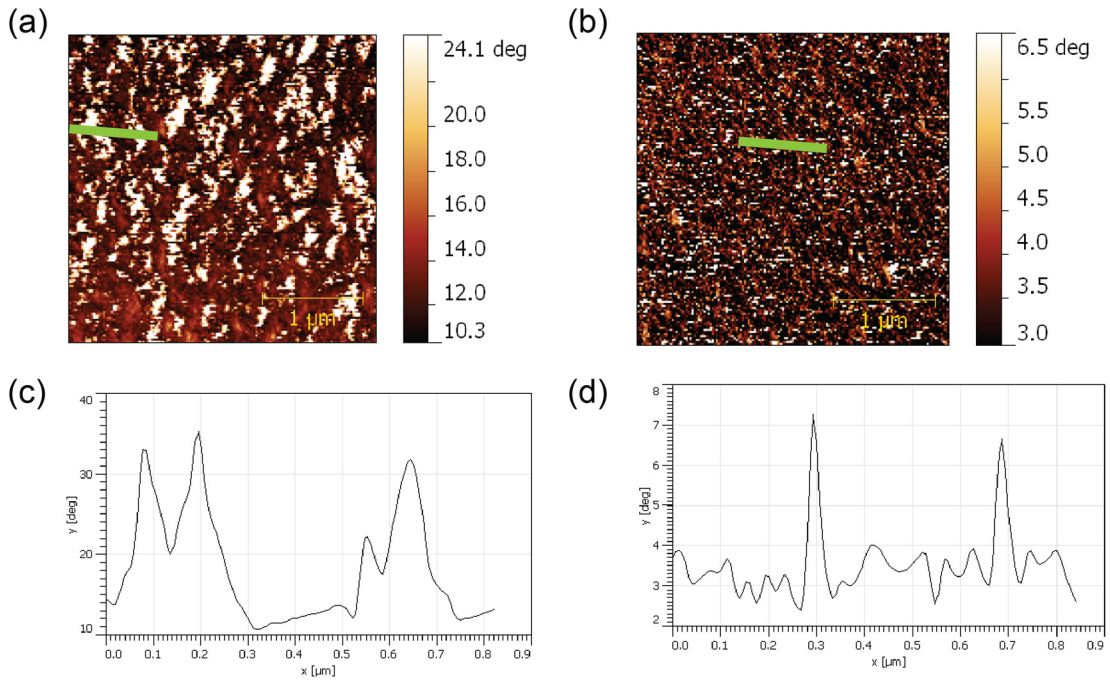

Figure S6. Phase images for (a) PTB7-hPDI2 and (b) a ternary PTB7-SWCNT-hPDI2 blend with 0.1 wt% SWCNTs. In each figure, a green line indicates the position where the line scans in (c) and (d) were taken, respectively.

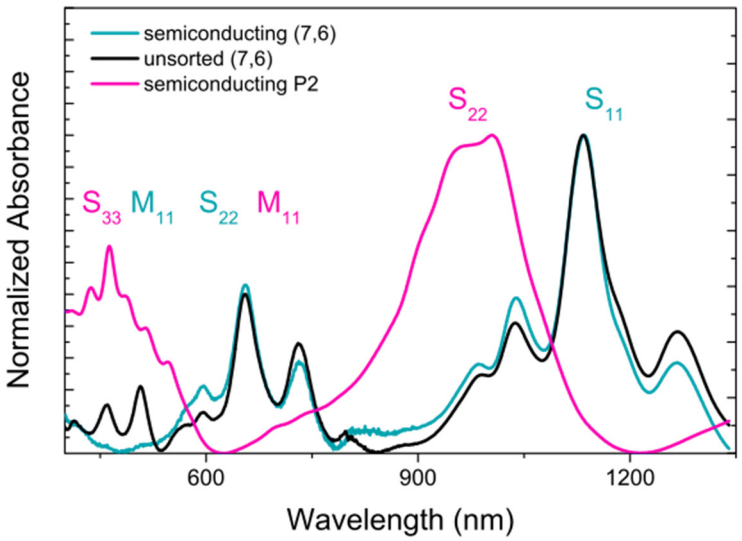

Figure S7. UV-Vis absorption spectra of unsorted (7,6) SWCNTs, 97% semiconducting (7,6) SWCNTs, and 98% semiconducting P2 SWCNTs. The semiconducting S_{22} and S_{33} and metallic M_{11} transitions are noted in red for the P2 large diameter SWCNTs. The semiconducting S_{11} and S_{22} and metallic M_{11} transitions are noted in blue for the (7,6) SWCNTs. The suppression of the M_{11} peaks in the semiconducting samples is indicative of high semiconducting purity. The unsorted (7,6) sample shows a strong presence of metallic SWCNTs.

Table S4. Summary of photovoltaic parameters for the solar cells shown in Figure 4 of the main text. Champion values listed in [brackets].

	Voc (V)	Jsc (mA/cm^2)	FF (%)	PCE (%)
No SWCNTs	0.70 ± 0.01 [0.72]	6.77 ± 0.15 [6.98]	35.9 ± 1.7 [36.6]	1.72 ± 0.06 [1.9]
(7,6) sSWCNTs	0.70 ± 0.01 [0.73]	9.17 ± 0.46 [9.78]	41.0 ± 1.6 [42.7]	2.61 ± 0.18 [3.0]
(7,6) uSWCNTs	0.68 ± 0.02 [0.70]	5.73 ± 0.36 [6.11]	41.2 ± 1.3 [42.0]	1.61 ± 0.17 [1.8]
P2 sSWCNTs	0.63 ± 0.01 [0.64]	7.70 ± 0.61 [8.48]	33.8 ± 1.2 [35.1]	1.62 ± 0.08 [1.9]

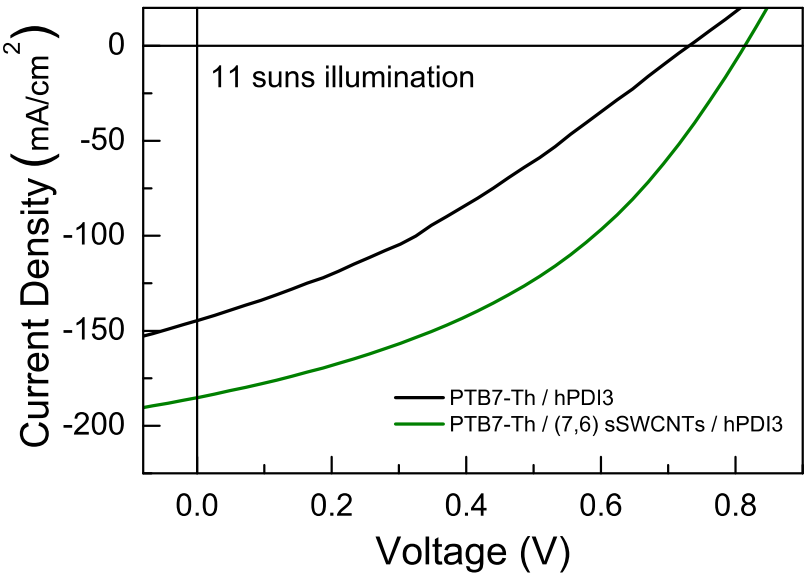

Figure S8. Current voltage curves of PTB7/hPDI3 with and without SWCNTs at 11 suns illumination.

Additional Experimental Methods

Active Layer Solution Preparation: Poly[[4,8-bis[(2-ethylhexyl)oxy]benzo[1,2-b:4,5-b']dithiophene-2,6-diyl][3-fluoro-2-[(2-ethylhexyl)carbonyl]thieno[3,4-b]thiophenediyl]] (PTB7) and Poly[4,8-bis(5-(2-ethylhexyl)thiophen-2-yl)benzo[1,2-b;4,5-b']dithiophene-2,6-diyl-alt-(4-(2-ethylhexyl)-3-fluorothieno[3,4-b]thiophene-)-2-carboxylate-2-6-diyl)] (PCE10 / PBDTTT-EFT / PTB7-Th) were purchased from Ossilla. Active layer solutions comprising PTB7 and PDI dimer with and without SWCNTs were fabricated by adding PTB7 and PDI dimer to CB at a 1:2 ratio with a total loading of 25 mg/mL and 1 vol% DIO. CB was replaced with the SWCNT-CB solutions described above to achieve the target SWCNT loading. Active layer solutions of PTB7-Th and PDI trimer were prepared analogously. All solutions were stirred for two days at 60 °C to completely dissolve all components.

Absorbance and Photoluminescence Measurements: UV-Vis optical absorbance spectroscopy measurements were taken with an Agilent Cary 5000 on films of individual active layer components spin-coated on ITO. Photoluminescence measurements were taken on single-layer or bilayer thin films on glass substrates. For polymer and small molecule photoluminescence, a 500 nm excitation wavelength was used with 5 nm slit width and 1 s integration time. For SWCNT photoluminescence, a 650 nm excitation was used with a 10 nm slit width and 60 s integration time. Measurements were taken on a Horiba Spectrometer with a low pass filter blocking the excitation light from the emission detector. Silicon and liquid-nitrogen cooled indium gallium arsenide detectors were used for the visible (polymer and small molecule) and near-infrared (SWCNT) emissions, respectively.

Device Fabrication: Pre-patterned indium tin oxide (ITO) glass substrates (1 × 2 in^2, 15 Ohm/Sq, Thin Film Devices) were cleaned by ultrasonic treatment in aqueous detergent (Alconox), deionized water, acetone, and isopropyl alcohol sequentially. ZnO layers were prepared by spin-coating 0.1 M of zinc acetate and ethanolamine in 2-methoxyethanol solution on ITO at 3,000 rpm for 60 sec followed by annealing at 200 °C for 60 min in air. To fabricate the photovoltaic devices, 20 μL of the active layer described above was spread across the ZnO nanowire substrates and spin-coated in an inert nitrogen atmosphere at 1,000 rpm for 60 sec. The films were subsequently annealed at 100 °C for 10 min. Next, the films were placed in a glovebox-enclosed thermal evaporator and pumped down to 5 x 10^{-6} Torr. Device fabrication was completed by depositing 7.5 nm of

molybdenum oxide (Alfa-Aesar, Puratronic 99.9995%) and 100 nm of silver (Lesker). A device area of 0.06 cm^2 was defined as the overlap between the patterned ITO, active layer, silver cathode, and a black mask affixed to the illuminated side of the device.

Device Evaluation: For 1 sun measurements, the completed devices were tested under 100 mW/cm^2 of calibrated solar simulated light from a Xenon arc lamp source (Newport) with an AM 1.5G filter. For higher illuminations, the source lamp was focused using lenses to a smaller spot size, and the intensity was calibrated using a silicon photovoltaic detector with a known efficiency by comparing the output short circuit current of the device. In all cases, the concentrated illumination size was larger than 1 cm^2. External quantum efficiency measurements were performed with a 75 W monochromated light source utilizing a Xenon arc lamp for the visible spectrum and a tungsten lamp for the near-infrared portion of the spectrum. Measurements were calibrated with a silicon photodetector. All measurements were taken using devices without encapsulation under ambient conditions.

Microscopy Characterization: Scanning electron microscopy (SEM) was used to analyze the surfaces of the carbon nanotube samples. For the SEM images, a Hitachi SU8030 series Ultra-High Resolution (UHR) Cold-Emission FE SEM was used with an applied voltage of 2.0 kV. Atomic force microscopy (AFM) was used to examine the active layer morphologies. AFM measurements were taken on an Asylum Research Cypher AFM using 300 kHz Si cantilevers in normal tapping mode.

References

1. Weisman, R. B.; Bachilo, S. M. Dependence of Optical Transition Energies on Structure for Single-Walled Carbon Nanotubes in Aqueous Suspension: An Empirical Kataura Plot. *Nano Lett* **3**, 1235-1238 (2003).